Structural analysis of Ba-induced surface reconstruction on Si(111) by means of core-level photoemission

Taichi Okuda
Synchrotron Radiation Laboratory, Institute for Solid State Physics (SRL-ISSP), The University of Tokyo, 5-1-5 Kashiwanoha, Kashiwa 277-8581, Japan

Ki-Seok An
Thin Film Materials Laboratory, Korea Research Institute of Chemical Technology, Yusung P. O. Box 107, Taejon 305-600, Korea

Ayumi Harasawa and Toyohiko Kinoshita
Synchrotron Radiation Laboratory, Institute for Solid State Physics, The University of Tokyo, 5-1-5 Kashiwanoha, Kashiwa 277-8581, Japan

(Received 28 September 2003; revised manuscript received 22 November 2004; published 17 February 2005)

The surface structures of the Ba-induced 3×1, 5×1, and 2×8 reconstructions on the Si(111) surface were investigated by means of Si 2*p* and Ba 4*d* core-level photoemission and the coverage was estimated by x-ray photoemission (XPS). In the Si 2*p* core-level spectrum of every reconstructed surface, three prominent surface components that are shifted to lower and higher binding energies from the bulk peak have been observed. In the case of the 3×1 surface, these surface components are well explained by the so-called honeycomb-chain-channel (HCC) model which is considered to be the most plausible structure for alkali-metal-induced 3×1 surfaces. The similarity of the core-level spectra between the 2×8 surface and the Ca- or Yb-induced 2×1 surface suggests that both the 2×8 and 2×1 surfaces have similar short range Si structures. The observed double component in the Ba 4*d* core-level spectra of the 5×1 and 2×8 surfaces implies the existence of more than one Ba adsorption configuration on these surfaces. Our estimated metal coverages by XPS for the 5×1 and 2×8 surfaces are ~0.2 and ~0.3 monolayers which are different from those of previous studies for the Ca/Si(111) system. On the basis of these results we proposed possible surface structural models for the 5×1 and 2×8-Ba surfaces based on a combination model of the HCC and Seiwatz chain structures. The intensity change of each Si 2*p* surface component and the other experimental results are qualitatively explained with the models.

DOI: 10.1103/PhysRevB.71.085317 PACS number(s): 68.35.−p, 68.43.−h, 73.20.−r

I. INTRODUCTION

One-dimensional (1D) nanostructures on semiconductor surfaces have attracted significant attention because of their interesting electronic properties caused by the 1D electronic structure as well as their potentials for nanoelectronic devices. Self-assembling 1D patterning is one of the promising ways to prepare multiple regular nanopatterns on solid surfaces at a time and it may be very suitable to make nanodevices practically. In order to use this kind of self-assembled 1D structure in real nanodevices, control of the length or width of the wire must be important. Alkaline-earth-metal-(AEM-) induced 1D structures on the Si(111) surface are one of such interesting systems; their wire width can be controlled by changing the metal coverage and the substrate temperature. In the case of Ca adsorption, for example, a variety of 1D reconstructions having different wire widths with $n\times1$ periodicity ($n=3$, 5, 7, 9, and 2) is observed for increasing Ca coverage.[1–4] In addition to Ca, other AEMs induce the $n\times1$ reconstructions [$n=3$ for Mg,[5] $n=3$ and 5 for Ba (Ref. 6)].

Among these $n\times1$ surface reconstructions, the 3×1 surface, the smallest coverage phase, has been investigated most extensively. This 3×1 reconstruction is commonly induced by a variety of metals having different valence electrons, such as monovalent alkali metals (AMs, Li, Na, K, Rb, Cs),[7–14] noble metals (Ag),[8,10,15] and divalent rare earth metals (REMs, Yb, Sm, Eu),[16–18] as well as AEMs. Through plenty of experimental and theoretical studies, the honeycomb-chain-channel (HCC) model is now believed to be the most plausible geometric structure for monovalent AM- and Ag-induced 3×1 surfaces.[19,20] In this model, AM or Ag atoms of 1/3 monolayer (ML; 1 ML = $7.83\times10^{14}/\mathrm{cm}^2$) form linear chains in the channels between honeycomb structures. This HCC model is energetically more stable than the other proposed models, and the calculated scanning tunneling microscopy (STM) images, surface core-level shift (SCLS) of the Si 2*p* level, and band dispersion having semiconducting character are in fully accordance with the experimental results.[19,20]

From the similar low-energy electron diffraction (LEED) *I-V* curves[8] and the STM images,[10,11] it had been suggested that the AEM-induced 3×1 surface has almost the same reconstruction with the same metal coverage (1/3 ML) as the AM- and Ag-induced 3×1 surfaces. If this is the case, the divalent AEM-induced 3×1 surface with $\theta=1/3$ ML should be metallic within the one-electronic picture due to the odd number of surface electrons in the unit cell (i.e., three Si dangling bonds and two electrons from the AEM). The surface electronic states observed by photoemission

studies,[2,5,21] however, are semiconducting. At the same time, in the atomically resolved STM images, a 3×2 periodicity was observed on the 3×1-Ca surface, while it was not observed in the LEED pattern.[1]

To understand the semiconducting character with the 3×2 periodicity, an electron correlation effect, such as the Mott transition or charge density wave (CDW), was suggested at first.[2,5] The other explanation attributed it to the different metal coverage of the AEM-induced 3×2 surfaces from AM-induced 3×1 surfaces.[21,22] That is, the metal coverage of $\theta=1/6$ ML in the 3×2-AEM surface leads to the same surface electron number as the 3×1-AM with $\theta=1/3$ ML, resulting in a semiconducting character of the 3×2-AEM surface within the one-electron picture.[21] Recently, an estimation of the absolute Ba coverage in the 3×2-Ba surface has been done by means of a medium-energy ion scattering study[22] and it confirmed the Ba coverage of $\theta=1/6$ ML on the 3×2-Ba surface. A coverage of $\theta=1/6$ ML has also been estimated on the Ca-induced 3×2 surface very recently.[4] These experimental results are also supported by theoretical studies. A recent first-principles calculation[23] shows that the HCC model with $\theta=1/6$ ML of an AEM is energetically the most stable compared with the HCC model with $\theta=1/3$ ML of an AEM or the other models with $\theta=1/6$ ML of an AEM, and the STM images and semiconducting band gap are also well reproduced by the model.[23]

Compared to the 3×1- (=3×2-)AEM surface, AEM induced other $n\times1(n=5,7,9,2)$ surfaces have not been investigated intensively. From the STM observations, it is proposed that the intermediate phases [$n=5$, 7,[2–4] and 9 (Ref. 4)] are formed by simple combinations of the HCC model having $\times3$ periodicity and a structure having $\times2$ periodicity.[2,3] The electronic structures of these Ca-induced intermediate phases were reported to be semiconducting by angle-integrated photoemission.[2] The STM images of the intermediate structures, however, are always unclear,[2,3,24] and the relation between electronic and atomic structures of the intermediate phases has not been established yet.

In the above mentioned model for the intermediate phase, the structure having 2×1 periodicity is assumed to be the so-called Seiwatz chain structure with $\theta=1/2$ ML metal coverage.[2,3] The semiconducting character of the 2×1-Ca surface observed by photoemission studies[2,25,26] is qualitatively consistent with the Seiwatz chain structure. At the present, however, it is not evident that the AEM-induced 2×1 reconstruction has the Seiwatz chain structure, and even the absolute coverage is not apparent. Unlike Ca and REMs (Yb and Eu), in the case of Ba adsorption, the highest-coverage phase observed by LEED is not the 2×1 but the 2×8.[6] The difference between the Ca- or REM-induced 2×1 and the Ba-induced 2×8 surface, however, is not clear and there is no study to investigate the difference between them, thus far.

In this paper, we present the results of surface-sensitive Si $2p$ and Ba $4d$ core-level photoemission of the Ba-induced 3×1, 5×1, and 2×8 reconstructions. From the analysis of the Si $2p$ surface core-level shifts, it is affirmed that the HCC model is plausible for the structure of the 3×1-Ba surface. The resemblance of the SCLSs between the 2×8 surface and the Ca- and Yb-induced 2×1 surfaces strongly suggests that they have quite similar short-range atomic structures. The intensity change of each surface component from the 3×1 to the 2×8 via the 5×1 structure is basically explained by a model that is a combination of the HCC and Seiwatz chain structures. In addition, the existence of two components in the Ba $4d$ core-level spectra of the 2×8 and 5×1 surfaces suggests that there is more than one Ba adsorption configuration in these reconstructed surfaces. On the basis of the Si $2p$ and Ba $4d$ core-level photoemission results, as well as the estimated Ba coverage by x-ray photoemission spectroscopy (XPS), we propose one possible structural model for the 5×1 and 2×8 surfaces.

II. EXPERIMENT

The high-resolution core-level measurements were performed mainly at the undulator beamline BL-16A, and XPS and work-function measurements were done at the bending magnet beamlines BL-18A and 1C of the Photon Factory in KEK (Tsukuba, Japan). Core-level spectra were recorded using the CL100(VSW) hemispherical analyzer with an acceptance cone of ±8° at the sample temperature of 110 K. For different surface-sensitive core-level measurements, we used several different photon energies ($h\nu=110$, 113, 115, 120, 130, 135, and 140 eV) and electron emission angles (0° and 60° from the surface normal). Since the angle between the incident light and the analyzer was fixed at 45°, the light incident angle is 45°(15°) from the sample normal direction when we measure normal (60°) emission. An n-type Si(111) wafer (20–30 Ω cm) was cleaned by direct current heating up to 1525 K in an ultrahigh-vacuum chamber at a base pressure of 2×10^{-8} Pa. The sample cleanliness was ascertained by the sharp 7×7 LEED pattern and the surface components of the core-level spectrum which are typical of the 7×7 clean surface.[27] Absence of the O 1s and C 1s peaks in the XPS spectra was also confirmed. Ba was evaporated from a thoroughly outgassed commercial getter source (SAES Getters) under a pressure of less than 3×10^{-7} Pa onto the clean sample at substrate temperatures of 1290, 1250, and 1120 K for the 3×1, 5×1, and 2×8 phases, respectively. This evaporation resulted in sharp 3×1, 5×1, and 2×8 LEED patterns as indicated in Fig. 1. After the evaporation, samples were cooled down immediately to 110 K for the high-resolution core-level photoemission measurement. The total energy resolution of the core-level measurements was 100–200 meV at 110 K depending on the photon energy. Work functions and coverages of Ba were estimated from the secondary electron cutoff energies and the Ba $3d$ and Si $2p$ XPS intensities.

III. RESULTS

Figures 1(a)–1(c) show the LEED patterns of the three Ba-induced phases (a) 3×1, (b) 5×1, and (c) 2×8. Although the intensity is very weak, faint streaks are visible in the pattern of the 3×1 phase at half-order lines as indicated by white arrows. Such half-order streaks have been observed on the Ca- or Yb-evaporated 3×1 surfaces more clearly.[1,4,28]

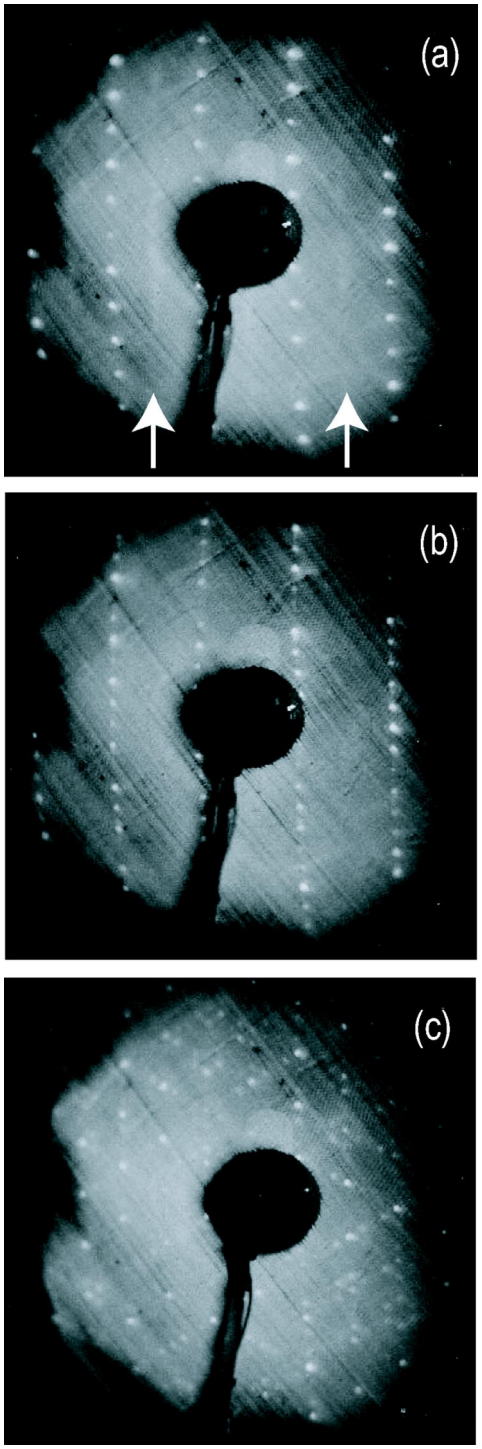

FIG. 1. Low-energy electron diffraction pattern of the Si(111) (a) 3×1, (b) 5×1, and (c) 2×8-Ba surfaces. Very weak streaks (indicated by white arrows) parallel to the $\times3$ spots at half of a $\times1$ periodicity in (a) indicate that the surface has actually a 3×2 periodicity.

The existence of these weak streaks reaffirms the recent STM findings that the AEM-induced 3×1 surfaces actually have a 3×2 periodicity.[1–3] Thus, we use the designation of 3×1-Ba for the Ba-induced reconstructed surface having 3×2 periodicity for simplicity, hereafter.

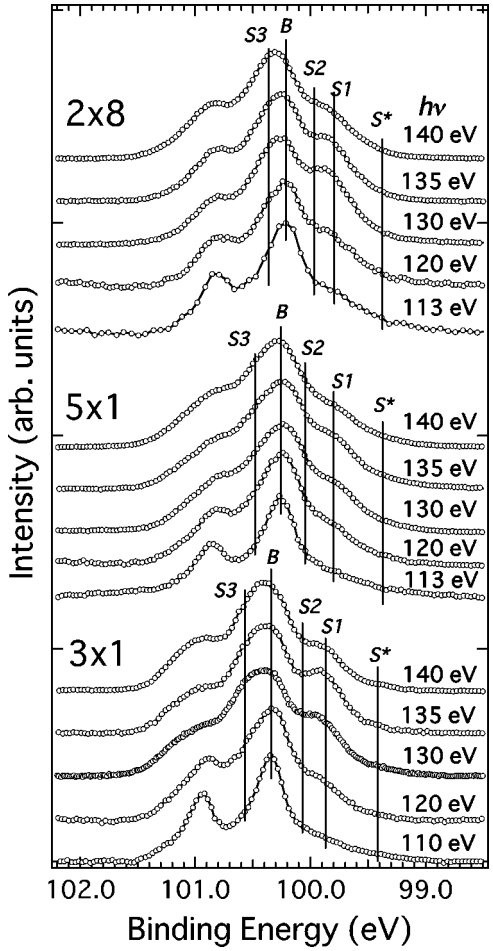

FIG. 2. Si $2p$ core-level spectra of the Ba/Si(111) surfaces measured with different $h\nu$ at 100 K in normal emission. The solid lines indicate the energy positions of the Si $2p_{3/2}$ parts of the four surface and one bulk components derived from the core-level fitting in Fig. 3.

The work functions[30] observed by photoemission cutoff (3×1, 3.44 ± 0.09 eV and 5×1, 3.22 ± 0.22 eV) are in good agreement with the microscopically analyzed work function for 3×1-Ba (3.0 ± 0.9 eV).[29] The (Ba $3d$)/(Si $2p$) XPS intensity ratios are 0.336 ± 0.047, 0.508 ± 0.017, and 0.58 for the 3×1, 5×1, and 2×8 phases. The change of intensity ratios is in good agreement with that observed by Weitering in an Auger electron spectroscopy measurement,[6] in which the Ba intensity changes 0.35, 0.5, and 0.65 for the 3×1, 5×1, and 2×8, respectively. Taking account of the metal coverage of $\theta=1/6$ ML for the 3×1 phase,[21–23] the XPS results lead to coverage of the 5×1 and 2×8 phases of 0.21–0.30 and 0.25–0.33 ML, respectively.

Figure 2 shows the Si $2p$ core-level spectra of the 3×1, 5×1, and 2×8 surfaces taken with different surface sensitivity, i.e., by different $h\nu$, at the surface normal direction and the sample temperature of 110 K. These spectra are normalized to the highest peak intensities. Because of the existence of several surface components (S_1–S_3 and S^*), which are deconvoluted as described later, surface-sensitive spectra ($h\nu=130$–140 eV) show characteristic shapes deviating from the bulk-sensitive spectra ($h\nu=110$ or 113 eV). That is,

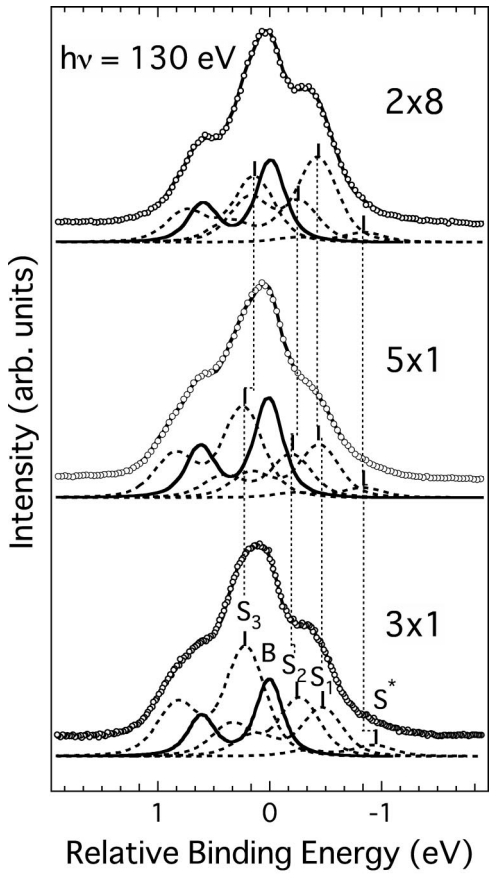

FIG. 3. Si $2p$ surface-sensitive core-level spectra of the 3×1, 5×1, and 2×8-Ba surfaces measured at $T_s=110$ K and $h\nu=130$ eV. Experimental spectra (open circles) are well reproduced by the convolution (thick solid curves) of the four surface components (labeled S_1, S_2, S_3, and S^*) and a bulk component (labeled B). The surface components and the bulk component are represented by dashed and thin solid curves.

in the spectra of 3×1, a flat shoulder or peak appears at the lower-binding-energy (E_B) side of the bulk peak. In addition, the main peak is broadened due to the high intensity of the surface state (S_3) at the higher-E_B side. In the 5×2 surface, the spectral shapes become more structureless and symmetric. The peak at the lower-E_B side of the 2×8 surface grows again and the spectral shapes become asymmetric. The shape of the main peak is, however, sharper than the other phases because of the shift of the S_3 state to the bulk peak position. As will be discussed later, the shape of the core-level spectra characteristic of each reconstruction changes a little depending on the photon energies due to the diffraction effect even though the spectra were measured with the angle-integrated photoelectron analyzer.

The observed core-level spectra were analyzed by a standard nonlinear least-squares fitting algorithm using Voigt functions. The fitting results of the representative surface-sensitive spectra taken at 130 eV with normal emission are presented in Fig. 3. In the curve fitting, the parameters of 608 meV for the spin-orbit splitting and 93 and 95 meV full width at half maximum (FWHM) for the Lorentzian contributions for all Si $2p$ 3/2 and 1/2 components were used. The

TABLE I. Relative energy shift of each surface component from the bulk component and the averaged intensity ratio of each component to the total surface intensity at different photon energies for the Ba/Si(111) systems.

	S^*	S_1	S_2	S_3
3×1 energy shift (meV)	−930	−474	−271	215
Intensity ratio	0.04	0.24	0.22	0.51
5×1 energy shift (meV)	−880	−453	−206	228
Intensity ratio	0.07	0.27	0.24	0.43
2×8 energy shift (meV)	−837	−420	−244	146
Intensity ratio	0.06	0.35	0.19	0.40

Gaussian widths were 134–182 meV (FWHM) for bulk components and 243–298 meV for surface components depending on measurements at different surface sensitivities. The intensity ratio of the $2p$ 1/2 to 3/2 component was changed slightly around the theoretical value $0.5(0.499\pm0.045)$. The credibility of these values was confirmed by the fitting of the 7×7 clean surface (not shown here) in which the fitting result is essentially consistent with those of previous high-resolution core-level measurements of the 7×7 surface.[27,31,32] As a result, every Ba-induced surface is well fitted with three prominent surface components (S_1, S_2, and S_3), a bulk component (B), and a very weak surface component (S^*), and the convoluted curves (thick solid curves) reproduce well the experimental data points (open circles). In every surface, S_1 and S_2 components shift to lower E_B's than the bulk peak B, and S_3 shifts to higher E_B than B. The shift of each component is not changed significantly in different phases as indicated by the dashed lines in Fig. 3. By using these components and the parameters, we could fit all of the core-level spectra having different surface sensitivities ($h\nu=110$, 113, 115, 120, 130, 135, and 140 eV, $\theta=0$, and 60°) without changing the energy shift of each component.

Table I summarizes the fitting parameters of each phase. In the table, as well as the energy shifts of surface components from the bulk component, the intensity ratios of each surface component to the total intensity of the surface components averaged over different surface sensitivities are presented. The change of the intensity ratio as a function of different surface reconstructions is more easily grasped in Fig. 4. As mentioned above and shown in Fig. 2, the intensity ratios of the surface components are affected by the diffraction effect and a little scattered. The range of the intensity variations of each component due to the diffraction effect in different photon energies is indicated by error bars in the figure. The tendency of each intensity ratio is, however, characteristic of each surface reconstruction. That is, in the 3×1 surface, the intensity ratio of S_1 and S_2 is nearly the same and that of S_3 is twice as large as each of them. The intensity ratio of S_3 decreases monotonically from 3×1 to 2×8 via the 5×1 phase. At the same time, that of $S_1(S_2)$ is almost constant in both the 3×1 and 5×1 phases but increases (decreases) in the 2×8 phase. As for the S^* state, the intensity ratio is almost constant.

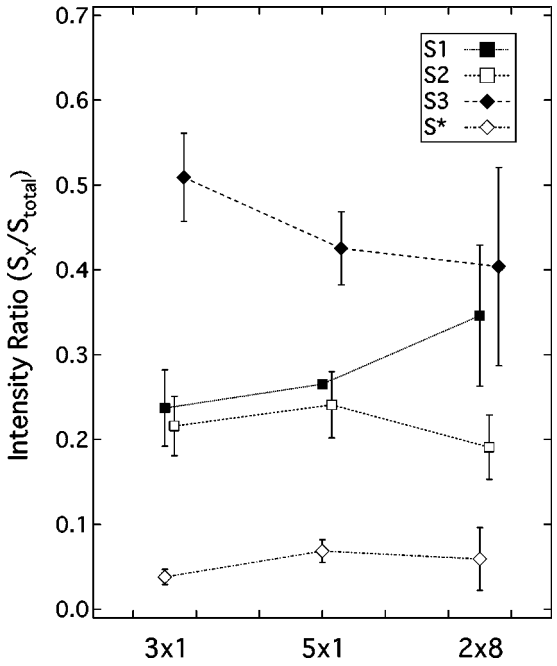

FIG. 4. Change of the intensity ratio of each surface component to the total intensity of surface components in the different surface reconstructions.

Figure 5 represents the Ba 4*d* spectra recorded at $h\nu = 140$ eV. The intensity ratio between the 4*d* 5/2 and 3/2 components deviates from the theoretical value (6:4), especially in the 3×1 and the 5×1 surfaces. The reason of the deviation is not evident at present but it may be due to the diffraction effect combined with the different initial and final states between 4*d* 5/2 and 3/2 components which was discussed in the In 4*d* core-level study in the In/Si(100) system.[33] The spectrum of the 3×1 surface is well reproduced by a single Ba 4*d* component with the Gaussian width (FWHM) of 291 meV and the Lorentzian width of 265 meV, respectively. On the contrary, the Ba 4*d* spectra of the 5×1 and the 2×8 surfaces cannot be fitted by a single 4*d* component with the same Gaussian and Lorentzian widths as those of the 3×1 surface. As a proof of the existence of multiple components, the spectrum of 2×8 shows a small shoulder at the lower-binding-energy side of the main peak. This result suggests that there is more than one Ba adsorption site on the 5×1 and 2×8 surfaces.

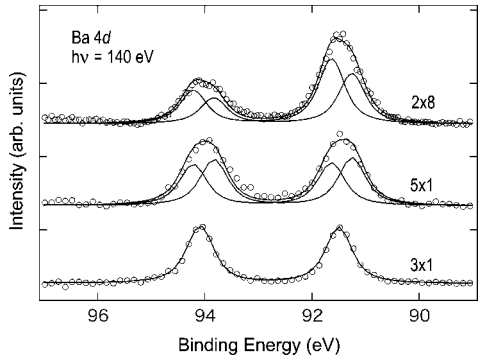

FIG. 5. Ba 4*d* core-level spectra of the 3×1, 5×1, and 2×8-Ba surfaces measured at $h\nu=140$ eV. Two components are required to fit the experimental spectra of the 5×1 and 2×8 surfaces, in contrast with the 3×1 surface in which only the one component can reproduce the experimental spectrum.

IV. DISCUSSION

A. 3×1 phase

From the wide range of experimental and theoretical studies, the Si structure of the lowest-coverage phase, the 3×1-(=3×2-) AEM, is considered to be almost the same as that of the AM-induced 3×1 surface, i.e., the HCC model. We present the structural model of the HCC model in the left hand side of Fig. 6(a). In the figure, AM atoms are indicated by small shaded circles and the topmost, second-layer, and third-layer Si atoms are represented by open, filled, and small filled circles, respectively. In the HCC model, metals are assumed to be positioned on the T_4 sites in channels formed by neighboring Si honeycomb chain structures. In the case of AM-induced 3×1 surface, since the coverage is $\theta=1/3$ ML, every T_4 site in the channel is occupied by an AM atom.

The fitting results of Si 2*p* core-level spectra of the 3×1-Na (Ref. 12) are well explained by the calculated SCLS of Kang and co-workers using the initial-state theory based on the HCC model.[20] According to the calculation, the surface component shifted to lower E_B than the bulk component originates from the Si atoms bonding with AM atoms [red and yellow circles in Fig. 6(a)]. As shown in the figure, these surface Si atoms are in a little different bonding configuration resulting in different energy shifts in the calculation. The other surface Si atoms making the double bonds (blue circles) in the honeycomb structure are assigned as the component shifted to higher E_B than the bulk peak. According to the calculation, the core-level shifts of these atoms making the double bond are approximately the same.

Our fitting results of the Si 2*p* state of the 3×1-Ba surface are in good agreement with the calculation for the 3×1-Na surface; namely, the S_1 and S_2 components shifted to lower E_B than the bulk component (B) in Fig. 3 correspond to the atoms indicated by red and yellow circles in the left hand side of Fig. 6(a). Correspondingly, the S_3 component shifted to higher E_B than B corresponds to the atoms indicated by blue circles. Regarding the intensity of each surface component, the observed intensity ratio ($S_1:S_2:S_3\sim1:1:2$) is also in good agreement with the assignment in which the intensity of the S_3 from two blue atoms should be twice as large as those of the S_1 and S_2 components from red and yellow atoms.

In the case of the AEM-adsorbed 3×1 phase, the coverage of 1/6 ML (half of the AM coverage) is strongly supported by recent experimental and theoretical studies.[21–23] Thus, it is considered that AEM atoms are located on every other T_4 site as indicated by large shaded circles in the right hand side of Fig. 6(a) and cause the 3×2 surface periodicity. In the model, the atomic structure of Si is the same as that of the AM-induced 3×1 model. However, the relative position between AEM atoms and the Si atoms labeled $\bar{a}$ is different from that of a in the 3×2 unit cell. As well as the a and $\bar{a}$

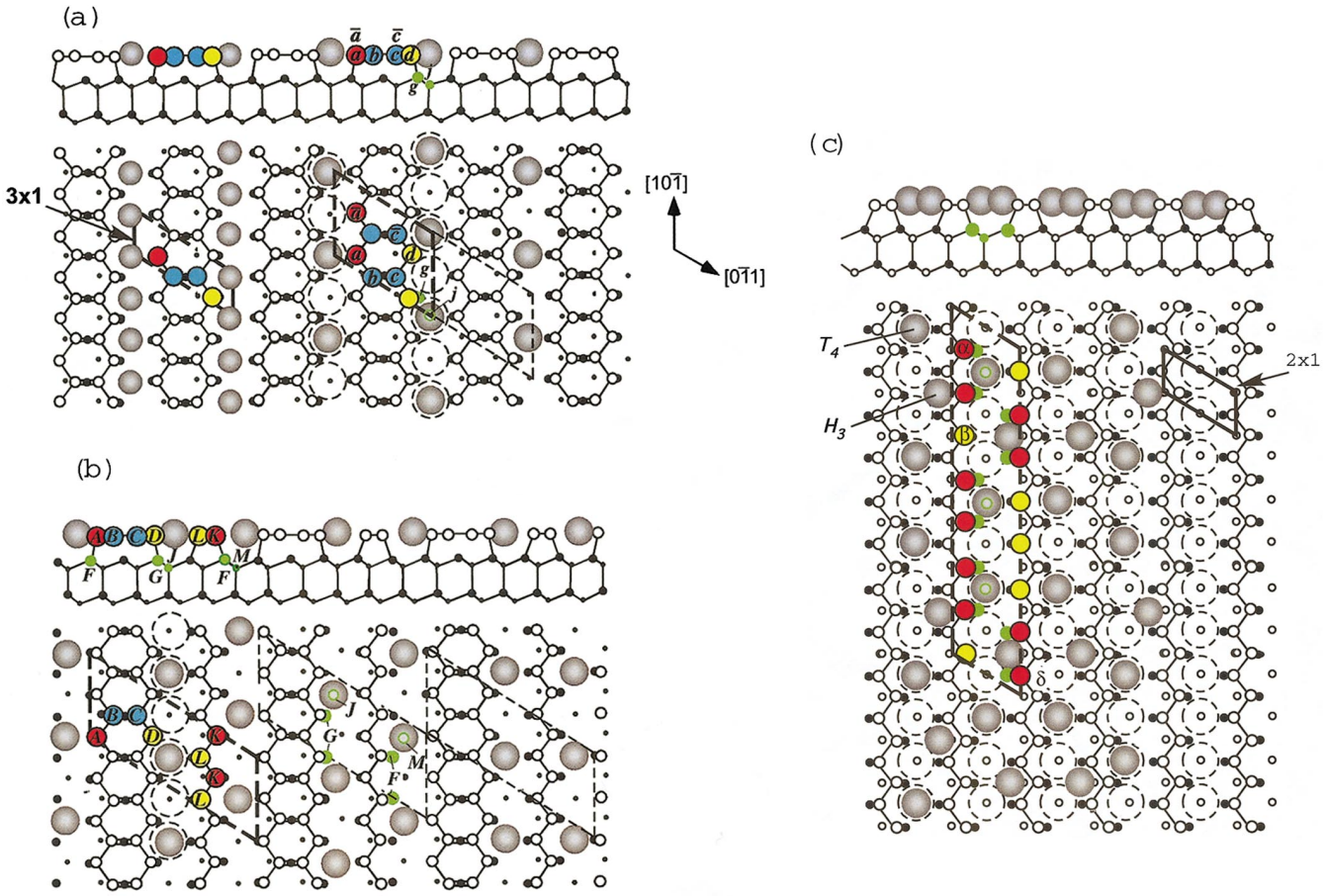

FIG. 6. (Color) Proposed surface structural models for the (a) 3×1, (b) 5×1, and (c) 2×8-Ba surfaces. The models are based on a simple combination model of the HCC and Seiwatz chain structures as proposed by several groups,[2,3] but modified in accordance with the results of the Si $2p$ and Ba $4d$ core-level fitting and the coverage estimation by XPS. The Ba and topmost Si atoms are indicated by the shaded circles and large open circles. Second- and third-layer Si atoms are represented by filled and small filled circles. Each parallelogram is the unit cell of each surface reconstruction.

atoms, the atoms labeled $\bar{c}$ and c are also in different configurations. Although these atoms in different configurations may cause different SCLSs in a simple consideration, our fitting result is surprisingly in good agreement with the calculation based on the HCC model with $\theta=1/3$ ML AM in which the a and $\bar{a}$ or c and $\bar{c}$ atoms are equivalent. The results suggest that the valence electron of the AEM is distributed almost equally to both the a and $\bar{a}$ or c and $\bar{c}$ atoms causing almost the same SCLSs of these two red or blue colored atoms. Similar surface state band structures of the 3×1-Ba to that of the 3×1-Na surface in a recent angle-resolved photoemission spectroscopy (ARPES) measurement[21] suggest that the chemical environment around surface Si atoms and their electronic states in the 3×2-AEM surface are quite similar to those of the 3×1-AM. Thereby, AEM atoms may behave as electron donors that donate two electrons to the Si substrate and make the HCC model stable rather than as adsorbates making strong covalent bonds with surface Si atoms. In other words, one electron in every 3×1 unit cell in average makes the HCC structure stable in both the 3×1-AM and 3×1-AEM surfaces.

The fitting results of a recent SCLS study of the 3×1-Ca surface[4] are almost consistent with our results, i.e., the number of prominent surface components and the amounts of shifts are almost the same in both the experiments. In the fitting results of the 3×1-Ca surface, however, the intensity ratio of S_2 is much smaller than that of S_1 in the measurement with some photon energies. From the intensity ratio, the authors of Ref. 4 assigned the surface components S_1 and S_2 as the a and d atoms, respectively, and the $\bar{a}$ atoms are excluded from the contribution to these surface components. Considering the environment of the $\bar{a}$ atoms, it seems to be a little bit unnatural that these atoms have almost the same core-level shift as the bulk atoms. The reason for the different intensity ratios between the present results and those of the Ca-induced 3×1 surface is not evident at present. Since their core-level spectra were recorded by an angle-resolved analyzer with a small acceptance cone,[4] the intensity ratio in their measurement may be affected much more by diffraction and the small intensity ratio of the S_2 may be caused by the diffraction effect.

As for the assignment of the surface components of the 3×1-Ca system, there is another calculation.[2] In the calculation, the assignment of the surface components ($=S_1$ and S_2) having lower E_B is consistent with our results although these two components are treated as one component in their

analysis. However, they have assigned the component with higher $E_B(=S_3)$ as the Si atoms under Ca atom [green small circles labeled *j* and *g* in the right hand side of Fig. 6(a)]. Because of the potential of the positively charged AEM atoms, it is natural that these atoms are more positively charged than bulk atoms and contribute to the S_3 components. However, considering the expected intensity reduction of the *j* and *g* atoms because of the short mean free path of the surface-sensitive measurement and the strong intensity of the S_3 component, which is twice as large as the other components, the contribution of the extra surface Si atoms such as the *b* and *c* atoms in addition to the atoms under AEM atoms seems to be necessary. As the authors pointed out in Ref. 2, in spite of the semiconducting character observed by photoemission spectroscopy, they assumed that the 3×1-Ca surface was a metallic surface in their calculation since they considered the Ca coverage is 1/3 ML for the 3×1-Ca surface. The over estimation of the screening effect in the calculation[2] may cause the different results from the calculations of Kang and co-workers.[20]

B. 2×8 phase

From LEED and STM observation, the surface structure of the AEM-induced highest-coverage phase is assumed to be the so-called Seiwatz chain structure.[2–4] This structure consists of dimerized Si chains as indicated in the right hand side of Fig. 6(c) and forms the 2×1 reconstruction. In the model, the locations of metals are assumed to be the T_4 sites (broken circles), and the metal coverage is $\theta=1/2$ ML. The semiconducting character observed in the recent ARPES studies[25,26] and the angle-integrated PES study[2] of the Ca-induced 2×1 surface is qualitatively consistent with a structure having an even number of electrons in the unit cell. In the case of Ba adsorption, however, the 2×8 reconstruction is observed as the highest-coverage phase instead of the 2×1.[6] The reason for the different surface reconstructions between Ba and other AEM adsorption is not evident. One of the explanations suggested by Weitering is that the AEM- or REM-induced highest-coverage phase commonly has the 2×8 structure but the high density of defects on the surfaces causes the eighth-order spots to vanish in the LEED pattern with a high background intensity. However, the clear LEED pattern of the 2×1-Ca with a very weak background[4] and the STM images with little defect[2] are inconsistent with the explanation.

It is worthwhile to note that the spectral shape and the fitting results of the Si 2*p* core level of the 2×8-Ba surface are quite similar to those of the Yb- and Ca-induced 2×1 surfaces.[2,4,16] The resemblance of the SCLSs strongly suggests that the short-range Si structure of 2×8-Ba is essentially the same as those of the other AEM- and REM-induced 2×1 surfaces. At the same time, the existence of multiple components in the Ba 4*d* core-level spectrum suggests that the Ba adsorption site is not only one as assumed in the simple Seiwatz chain structure. Therefore, we consider that the structure of the 2×8-Ba surface is a modified structure of the 2×1 structure, i.e., a modified Seiwatz chain structure. In the case of the original Seiwatz chain structure, the metal coverage is considered to be $\theta=1/2$ ML. The coverage of 2×8-Ba($\theta=0.25-0.33$ ML) estimated by our XPS measurement, however, was considerably smaller than $\theta=1/2$ ML. Although it is not evident that the coverage of 2×1-Ca is $\theta=1/2$ ML, because of the larger size of the Ba than the other AEMs, they probably cannot occupy every T_4 site in the channel of the Seiwatz chain structure resulting in a lower coverage and causing the 2×8 periodicity. From the estimated coverage of $\theta\sim0.3$ ML, the number of Ba atoms in the 2×8 unit cell can be calculated as about five. Furthermore, considering the fitting results of Ba 4*d* in which the intensity ratio of the two components is 1:0.8, these two components may correspond to three and two Ba atoms.

In accordance with the estimation and the results of the Si 2*p* SCLS, we tentatively propose one possible structural model for the 2×8 surface as indicated in Fig. 6(c). This model consists of the Si substrate having the same reconstruction as the original Seiwatz chain structure and Ba atoms with $\theta=0.3$ ML. In the 2×8 unit cell (parallelogram), Ba atoms are located at three T_4 sites and two H_3 sites in the light of the aforementioned XPS and Ba 4*d* core-level results. Since the exact order of the T_4 and H_3 sites is not evident, we positioned them tentatively. Because of the different kinds of sites, the Ba 4*d* core-level spectrum can contain two components. The modification of Ba positions from the original Seiwatz chain structure makes a $\times8$ periodicity along the dimer row. Thus, in this model, the $\times2$ periodicity of the Seiwatz chain structure of the Si substrate and the $\times8$ modulation caused by the Ba adsorption make a 2×8 periodicity.

C. 5×1 phase

As for the structures of the intermediate phases, a concept for the series of reconstructions (3×1, 5×1, $7\times1,\ldots,2\times1$) was proposed by two different groups based on STM observation.[2,3] The fundamental concept of the model is that the intermediate phases consist of simple combinations of the 3×1 (HCC) and the 2×1 (Seiwatz chain) structures. Figure 6(b) is our proposed possible structural model for the 5×1-Ba surface on the basis of the concept. In this model, the Ba atoms are located at every other T_4 site and the coverage is 0.2 ML, approximately consistent with our XPS results ($\theta=0.21-0.30$ ML). Since both the structural units have $\times2$ periodicity along the $[10\bar{1}]$ direction the surface has actually a 5×2 periodicity. In our LEED pattern of the 5×1 surface, however, there is no sign of existence of a $\times2$ periodicity. As shown in Fig. 6(b), the shift of the Ba row along $[10\bar{1}]$ can be more random (see the three kinds of parallelograms) than the $3\times1(=3\times2)$ surface [see the thick and thin broken parallelograms in Fig. 6(a)]. As indicated by the LEED simulation of the 3×1-Ba($=3\times2$-Ba),[34] considering the possible higher randomness in the registration of the $5\times1(=5\times2)$ surface, the $\times2$ LEED spots (or streaks) may vanish in our LEED observation. In addition, very recently, in the LEED pattern of the 5×1-Ca surface at low temperature, very faint spots originating from the 5×2 periodicity have been observed.[4] Therefore we believe that the local structure of the 5×1-Ba surface has actually a 5×2

periodicity. (Note, we use the notation, 5×1, rather than 5×2 for simplicity hereafter.)

The fitting results of the Ba 4*d* core-level spectrum imply that there are also two kinds of Ba sites with almost the same occupation ratio on the 5×1 surface. In the model, because of the asymmetric Si structure, the environments around Ba in neighboring rows are different from each other even if the only Ba site is the T_4 site. Thus, the existence of two kinds of Ba core levels can be explained without considering the different sites of Ba atoms. In the recently proposed structural model for the 5×1-(=5×2-)Ca with $\theta=0.3$ ML,[4] Ca atoms are assumed to occupy every T_4 site in one row and every other T_4 site in the other row, as indicated by broken circles in the left side of Fig. 6(b). However, in this case, the expected intensity ratio of the two Ba components is 2:1 and inconsistent with our fitting results for the Ba 4*d* surface.

D. Interpretation of the SCLS of the Si 2*p* state

The results of the Si 2*p* SCLS can be explained qualitatively by these proposed models. As shown in Figs. 3 and 4, the intensity ratio of the S_3 component decreases monotonically from 3×1 to 2×8 via the 5×1 phase. Since the S_3 state in the HCC model is assigned as the double-bonding *b* and *c* atoms making the honeycomb structure in the calculation of Kang and co-workers,[20] the successive decrease of the honeycomb structure from the 3×1 to the 2×8 in these models is consistent with the reduction of the S_3 intensity ratio. In this assignment, however, the intensity of the S_3 component of the 2×8 phase should be zero if the component consists of only the double-bonding Si atoms. The residual intensity of the S_3 component even in the 2×8 surface suggests that the S_3 component includes the contribution of other atoms such as atoms underneath the Ba atoms (green circles in Fig. 6) as discussed in the preceding section. Considering the similar configurations of these green atoms (*g* and *j* of the 3×1, *G*, *J*, *F*, and *M* of the 5×1, and green circles of the 2×8), we assume a similar CLS for these surface atoms. In this assumption, the numbers of the atoms underneath Ba which may contribute to the S_3 state are 3, 6, and 10 in the 3×1, 5×1, and 2×8 unit cells. Although, in the 2×8 model, the order of the T_4 and H_3 sites is not evident, the number of green atoms in the unit cell is always 10. Thus, the contribution of the atoms underneath Ba to the S_3 components changes as 3/6, 6/10, and 10/16 (=0.5, 0.6, and 0.625) for the 3×1, 5×1, and 2×8 surfaces. Taking account of the intensity reduction due to the finite penetration depth of the electrons, the contribution of the atoms underneath Ba should be smaller than that of the atoms forming the honeycomb structure. Therefore, in this interpretation, the intensity of the S_3 component which is the sum of these contributions decreases from the 3×1 to 2×8 via 5×1 but does not become zero. In addition, the slight change of the energy position of the S_3 component in the 2×8 surface from those of the other reconstructions may reflect that the S_3 component in the 2×8 surface consists of only the Si atoms under the Ba atoms in contrast with those in the 3×1 and the 5×1 surfaces in which the contributions from the Si atoms of both the honeycomb structure and the underneath Ba are included.

It is more difficult to assign the S_2 and S_1 components in the 5×1 and 2×8 surfaces. The assignment of the atoms making the zigzag chain which exists in both the 5×1 and 2×8 structures is not evident. In previous SCLS studies of 2×1-Ca, Baski *et al.* assigned the Si atoms neighboring AEM atoms [red colored atoms labeled α in Fig. 6(c)] as the S_1 component based on their calculation, although the S_2 component is not resolved from the bulk component in their study.[2] The dominant S_1 component for the 2×8 surface in Fig. 3 is in agreement with their observed surface component and we infer the component as the red colored Si atoms labeled α. In the same analogy, the atoms labeled *K* in the 5×1 model can be assigned as S_1 of the 5×1 surface.

As seen in Figs. 6(b) and 6(c), the Si atoms labeled *L* and β (yellow colored atoms) in the zigzag chain are a little far from Ba atoms compared with the α and *K* atoms. Due to the weaker influence of the Ba atoms in these Si atoms, the energy shift of these surface atoms may be smaller than those of the α and *K* atoms. Thus, these atoms in the zigzag chain may contribute to the S_2 components. The larger intensity of S_1 than S_2 in the 2×8 surface is consistent with the assignment.

Considering the similar chemical environment, the *A* and *D* atoms in the honeycomb structure of the 5×1 model should have a similar core-level shift to those of the *a* and *d* atoms in the 3×1 surface and contribute to the S_1 and S_2 components in addition to the aforementioned *K* and *L* atoms. Thus, the number of atoms that contribute to S_1 and S_2 in the 5×1 model is roughly the same ($S_1=K$ and *A*, $S_2=L$ and *D*), being consistent with the observed intensity ratio of the S_1 and S_2.

Finally, we discuss a little the faint component S^*. This S^* component is observed in every phase in the lowest- E_B region. In the previous SCLS studies of the Ca/Si(111) system,[2,4] a similar component was also observed. Sakamoto and co-workers assigned the component as the intrinsic component of the 5×1 structure since they did not observe the similar component in the 3×2 and 2×1-Ca surfaces.[4] In the present core-level study, however, we observe the S^* component in every surface reconstruction. In a SCLS study of the Ba-deposited Si(001) surface at room temperature, the surface component originating from the formation of Ba monosilicide has been observed at the energy range of -0.8 to -1.0 eV from the bulk component.[35] When the sample is annealed, it is considered that the formation of the silicide is more likely to occur. The formation of Ca silicide on Si(111) is frequently observed.[1,3] In addition the STM images of intermediate phases (5×1, 7×1,…) are always not clear and in high-resolution images many defectlike structures have been observed.[2,3] Therefore, from the E_B shifts similar to those of the Ba monosilicide and the above mentioned considerations we infer that the S^* component is due to a small portion of Ba silicide or a defect structure.

V. CONCLUSION

The structures of the Ba-induced reconstructions (3×1, 5×1, and 2×8) on the Si(111) surface have been investigated by spectroscopic measurements such as surface-

sensitive core-level spectroscopy of Si 2*p* and Ba 4*d* and XPS. The fitting results of the Si 2*p* and Ba 4*d* core levels reconfirmed that the surface structure of the 3×1 (which is actually the 3×2) is in good agreement with the honeycomb-chain-channel model. From the similarity of the Si 2*p* core-level spectrum, the short-range Si structure of the 2×8 surface must be almost the same as that of the 2×1-Ca or -Yb surface. The observed double component in the Ba 4*d* core levels of the 5×1 and 2×8 surfaces strongly suggests the existence of multiple Ba adsorption configurations on these surfaces. Considering the estimated Ba coverage, which is different from that in the Ca/Si(111) system, as well as the results of the Si 2*p* and Ba 4*d* core levels, modified structural models are proposed for the Ba-induced 5×1 (which is actually the 5×2) and 2×8 surfaces based on previously proposed models which are a combination of the HCC and the Seiwatz chain models. In the model of the 2×8 surface, two different Ba adsorption sites, T_4 and H_3 sites, play an important role to form a 2×8 periodicity. With these models, we can explain the change of the Si 2*p* core-level spectra qualitatively. In order to verify the proposed models as well as the origin of the 2×8 structure for Ba adsorption, atomically resolved STM observation and theoretical calculations of the core levels and valence electronic structures for the Ba-induced reconstructions are expected.

ACKNOWLEDGMENTS

The authors would like to thank the staff of the Photon Factory, especially Dr. J. Adachi and Dr. K. Ito for their support in the experiment. We also appreciate Dr. Y. Yamashita, Dr. S. Machida, and Professor J. Yoshinobu for their kind help in the experimental setting. T.O. is grateful to S. Nakazono and K. Nakamura for their help in the experiment. This study was supported in part by a Grant in Aid for Creative Basic Research from the Ministry of Education, Science, Sports and Culture of Japan. This work was performed under the Photon Factory Proposal No. 2000G006.

[1] A. A. Saranin, V. G. Lifshits, K. V. Ignatovich, H. Bethge, R. Kayser, H. Goldbach, A. Klust, J. Wollschlager, and M. Henzler, Surf. Sci. **448**, 87 (2000).
[2] A. A. Baski, S. C. Erwin, M. S. Turner, K. M. Jones, J. W. Dickinson, and J. A. Carlisle, Surf. Sci. **476**, 22 (2001).
[3] T. Sekiguchi, F. Shimokoshi, T. Nagao, and S. Hasegawa, Surf. Sci. **493**, 148 (2001).
[4] K. Sakamoto, W. Takeyama, H. M. Zhang, and R. I. G. Uhrberg, Phys. Rev. B **66**, 165319 (2002).
[5] K. S. An, R. J. Park, J. S. Kim, C. Y. Park, C. Y. Kim, J. W. Chung, T. Abukawa, S. Kono, T. Kinoshita, A. Kakizaki, and T. Ishii, Surf. Sci. **337**, L789 (1995).
[6] H. H. Weitering, Surf. Sci. **355**, L271 (1996).
[7] H. Daimon and S. Ino, Surf. Sci. **164**, 320 (1985).
[8] W. C. Fan and A. Ignatiev, Phys. Rev. B **41**, 3592 (1990).
[9] M. Tikhov, L. Surnev, and M. Kiskinova, Phys. Rev. B **44**, 3222 (1991).
[10] K. J. Wan, X. F. Lin, and J. Nogami, Phys. Rev. B **46**, 13 635 (1992).
[11] D. Jeon, T. Hashizume, T. Sakurai, and R. F. Willis, Phys. Rev. Lett. **69**, 1419 (1992).
[12] T. Okuda, H. Shigeoka, H. Daimon, S. Suga, T. Kinoshita, and A. Kakizaki, Surf. Sci. **321**, 105 (1994).
[13] K. Sakamoto, T. Okuda, H. Nishimoto, H. Daimon, S. Suga, T. Kinoshita, and A. Kakizaki, Phys. Rev. B **50**, 1725 (1994).
[14] T. Hashizume, M. Kayama, D. Jeon, M. Aono, and T. Sakurai, Jpn. J. Appl. Phys., Part 2 **32**, L1263 (1993).
[15] T. Fukuda, Phys. Rev. B **50**, 1969 (1994).
[16] C. Wigren, J. N. Andersen, R. Nyholm, U. O. Karlsson, J. Nogami, A. A. Baski, and C. F. Quate, Phys. Rev. B **47**, 9663 (1993).
[17] C. Wigren, J. N. Andersen, R. Nyholm, M. Göthelid, M. Hammar, C. Törnevik, and U. O. Karlsson, Phys. Rev. B **48**, 11 014 (1993).
[18] T. V. Krachino, M. V. Kuz'min, M. V. Loginov, and M. A. Mittsev, Appl. Surf. Sci. **182**, 115 (2001).
[19] S. C. Erwin and H. H. Weitering, Phys. Rev. Lett. **81**, 2296 (1998).
[20] M-H. Kang, J-H. Kang, and S. Jeong, Phys. Rev. B **58**, R13 359 (1998).
[21] T. Okuda, H. Ashima, H. Takeda, K-S. An, A. Harasawa, and T. Kinoshita, Phys. Rev. B **64**, 165312 (2001).
[22] G. Lee, S. Hong, H. Kim, D. Shin, J-Y. Koo, H-I. Lee, and Dae-Won Moon, Phys. Rev. Lett. **87**, 056104 (2001).
[23] S. Hong, H. Kim, G. Lee, J-Y. Koo, and H. Yi, J. Phys. Soc. Jpn. **71**, 2761 (2002).
[24] M. Aono, Y. Fukui, T. Urano, K. Ojima, and M. Yoshimura, Surf. Sci. **507-510**, 417 (2002).
[25] K. Sakamoto, H. M. Zhang, and R. I. G. Uhrberg, Phys. Rev. B **68**, 245316 (2003).
[26] Y. K. Kim, J. W. Kim, H. S. Lee, Y. J. Kim, and H. W. Yeom, Phys. Rev. B **68**, 245312 (2003).
[27] For example, C. J. Karlsson, E. Landemark, Y.-C. Chao, and R. I. G. Uhrberg, Phys. Rev. B **50**, R5767 (1994).
[28] R.-L. Vaara, M. Kuzmin, R. E. Perälä, P. Laukkanen, and I. J. Väyrynen, Surf. Sci. **529**, L229 (2003).
[29] M. Komai, M. Sasaki, R. Ozawa, and S. Yamamoto, Appl. Surf. Sci. **146**, 158 (1999).
[30] We did not measure the work function of the 2×8 surface in this study.
[31] J. J. Paggel, W. Theis, K. Horn, Ch. Jung, C. Hellwig, and H. Petersen, Phys. Rev. B **50**, 18 686 (1994).
[32] G. Le Lay, M. Göthelid, T. M. Grehk, M. Björkquist, U. O. Karlsson, and V. Yu. Aristov, Phys. Rev. B **50**, 14 277 (1994).
[33] H. W. Yeom, T. Abukawa, Y. Takakuwa, S. Fujimori, T. Okane, Y. Ogura, T. Miura, S. Sato, A. Kakizaki, and S. Kono, Surf. Sci. **395**, L236 (1998).
[34] J. Schäfer, S. C. Erwin, M. Hansmann, Z. Song, E. Rotenberg, S. D. Kevan, C. S. Hellberg, and K. Horn, Phys. Rev. B **67**, 085411 (2003).
[35] C.-P. Cheng, I.-H. Hong, and T.-W. Pi, Phys. Rev. B **58**, 4066 (1998).